The effect of demographic correlations on the stochastic population dynamics of perennial plants

Aldo Compagnoni,[1,9] Andrew J. Bibian,[1] Brad M. Ochocki,[1] Haldre S. Rogers,[1,7] Emily L. Schultz,[1] Michelle E. Sneck,[1] Bret D. Elderd,[2] Amy M. Iler,[3,4,8] David W. Inouye,[4,5] Hans Jacquemyn,[6] and Tom E. X. Miller[1]

[1]*Department of BioSciences, Program in Ecology and Evolutionary Biology, Rice University, 6100 Main Street, MS-170, Houston, Texas 77005 USA*
[2]*Department of Biological Sciences, Louisiana State University, Baton Rouge, Louisiana 70808 USA*
[3]*Aarhus Institute of Advanced Studies, Aarhus University, Høegh-Guldbergs Gade 6B, DK-8000, Aarhus C, Denmark*
[4]*Rocky Mountain Biological Laboratory, P.O. Box 519, Crested Butte, Colorado 81224 USA*
[5]*Department of Biology, University of Maryland, College Park, Maryland 20742 USA*
[6]*Division of Plant Ecology and Systematics, Biology Department, University of Leuven, Arenbergpark 31, B-3001, Heverlee, Belgium*

Abstract. Understanding the influence of environmental variability on population dynamics is a fundamental goal of ecology. Theory suggests that, for populations in variable environments, temporal correlations between demographic vital rates (e.g., growth, survival, reproduction) can increase (if positive) or decrease (if negative) the variability of year-to-year population growth. Because this variability generally decreases long-term population viability, vital rate correlations may importantly affect population dynamics in stochastic environments. Despite long-standing theoretical interest, it is unclear whether vital rate correlations are common in nature, whether their directions are predominantly negative or positive, and whether they are of sufficient magnitude to warrant broad consideration in studies of stochastic population dynamics. We used long-term demographic data for three perennial plant species, hierarchical Bayesian parameterization of population projection models, and stochastic simulations to address the following questions: (1) What are the sign, magnitude, and uncertainty of temporal correlations between vital rates? (2) How do specific pairwise correlations affect the year-to-year variability of population growth? (3) Does the net effect of all vital rate correlations increase or decrease year-to-year variability? (4) What is the net effect of vital rate correlations on the long-term stochastic population growth rate (λ_s)? We found only four moderate to strong correlations, both positive and negative in sign, across all species and vital rate pairs; otherwise, correlations were generally weak in magnitude and variable in sign. The net effect of vital rate correlations ranged from a slight decrease to an increase in the year-to-year variability of population growth, with average changes in variance ranging from −1% to +22%. However, vital rate correlations caused virtually no change in the estimates of λ_s (mean effects ranging from −0.01% to +0.17%). Therefore, the proportional changes in the variance of population growth caused by demographic correlations were too small on an absolute scale to importantly affect population growth and viability. We conclude that, in our three focal populations and perhaps more generally, vital rate correlations have little effect on stochastic population dynamics. This may be good news for population ecologists, because estimating vital rate correlations and incorporating them into population models can be data intensive and technically challenging.

Key words: demographic buffering; demographic correlation; environmental stochasticity; generalized linear mixed models (GLMM); hierarchical Bayes; integral projection model (IPM); stochastic population growth rate.

Introduction

In recent years, ecologists have become increasingly aware of the effects of temporal variability on population dynamics. This is a timely topic in global change ecology

(e.g., Jenouvrier et al. 2012, Vasseur et al. 2014, Lawson et al. 2015) because global circulation models suggest that climatic variability will increase (Easterling et al. 2000, Rahmstorf and Coumou 2011). Beyond its significance in the context of global change, temporal variability is a broadly important topic in ecology because its implications extend to evolutionary (Tuljapurkar et al. 2009), community (Adler et al. 2006), and ecosystem (Hsu et al. 2012) levels.

Theory predicts that temporal variability should generally decrease the long-term population growth rate (Lewontin and Cohen 1969, Tuljapurkar and Orzack

1980, Boyce et al. 2006). Consider that population size N grows from time t to $t + 1$ as a factor of the temporally varying geometric population growth rate λ_t, such that $N_{t+1} = N_t \lambda_t$. If λ_t is a random variable with expected value (arithmetic mean) $E[\lambda_t]$ and variance $\text{Var}(\lambda_t)$, the long-term stochastic population growth rate λ_s is approximated by $\log(\lambda_s) \approx \log(E[\lambda_t]) - \text{Var}(\lambda_t)/(2E[\lambda_t]^2)$ (Lewontin and Cohen 1969). Thus, an increase in variability is expected to decrease long-term population growth, all else equal. This expectation holds for both unstructured (Lewontin and Cohen 1969) and structured populations (Tuljapurkar and Orzack 1980, Fieberg and Ellner 2001) and is supported by empirical studies (e.g., Morris et al. 2008, 2011, Buckley et al. 2010, Jongejans et al. 2010).

Population growth is determined by a combination of individual-level demographic rates (e.g., survival, growth, and reproduction), henceforth called "vital rates," each of which can exhibit a unique pattern of temporal variation and covariation with other vital rates. Theory suggests that the sign and magnitude of correlations among vital rates is an important factor in determining the effect of temporal variability on population dynamics; this can be seen by expanding $\text{Var}(\lambda_t)$ to its lower-level variances and covariances (Tuljapurkar 1982). Positive correlation of vital rates through time (e.g., years that are bad for reproduction are also bad for survival) is expected to increase the variability in population growth, making the effect of temporal variance on the long-term stochastic growth rate (λ_s) more negative than if vital rates varied independently. Such positive temporal correlations could arise if vital rates exhibit similar responses to environmental forcing or extreme years (Doak and Morris 2010). On the other hand, negative correlation through time (e.g., years that are good for reproduction are bad for survival, and vice versa) is expected to decrease the variability of population growth, thereby buffering the negative effect of temporal variance on the long-term stochastic growth rate. Such negative temporal correlations could arise from life history trade-offs, such as those between reproductive and somatic function (Stearns 1992, Charnov 1993, Roff 2002). For example, costs of reproduction in plants could make years that are favorable for flowering unfavorable for growth, and vice versa (Williams et al. 2015). Negative correlation between vital rates may also reflect independent but opposing responses to environmental drivers, with no underlying trade-off between them (Knops et al. 2007).

Regardless of the underlying mechanisms, empirical understanding of vital rate correlations and their influence on stochastic population dynamics lags behind theory. A handful of empirical studies have suggested that vital rate correlations can be an important component of demographic variability (Coulson et al. 2005, Ezard et al. 2006, Evans et al. 2010, Jongejans et al. 2010, Morris et al. 2011, Jacquemyn et al. 2012, Davison et al. 2013, Elderd and Miller 2016). However, several challenges limit the ability to understand whether vital rate correlations deserve broader consideration in studies of stochastic population dynamics. First, demographic studies rarely exceed five interannual transitions (e.g., Salguero-Gómez et al. 2015). Limited temporal replication limits estimation because correlation coefficients are highly sensitive to sample size (Schönbrodt and Perugini 2013). For example, the majority of data sets analyzed by Jongejans et al. (2010), one of the most comprehensive studies of vital rate correlations to date, included between three and five transition years. These authors concluded that vital rate correlations rarely affected population growth in stochastic environments, but their power to estimate correlations was low. Second, even with sufficient data, accurately estimating vital rate correlations poses non-trivial technical difficulties. In particular, independent estimation of correlations and variances is required to model environmental stochasticity correctly (Doak et al. 2005). Moreover, there is no consensus regarding the best approaches for estimating vital rate correlations and their influence on population dynamics (e.g., Evans and Holsinger 2012).

Here, we use hierarchical Bayesian methods to quantify year-to-year vital rate correlations and population projection models to evaluate their contributions to stochastic population dynamics for three perennial plant populations. Our data sets span 11–15 years of demographic observations, providing an unusually strong empirical foundation for quantifying temporal variation and covariation in vital rates. We investigate the role of vital rate correlations in stochastic population dynamics by parameterizing population projection models with a set of generalized linear mixed models (GLMM). In this framework, year-specific vital rates are drawn from a multivariate distribution, thus linking the temporal fluctuations of different vital rates. To our knowledge, this is the first study to estimate vital rate correlations in this way, and the distinction carries several important advantages. First, each GLMM has direct correspondence to a particular life history process (growth, survival, fertility, etc.). Therefore, a linked GLMM framework facilitates biological interpretation by allowing us to test for correlations between life history functions *per se*. This approach contrasts with element-by-element parameterization of matrix models, where correlations between matrix elements may lack an intuitive biological interpretation. Second, the efficiency of a GLMM foundation reduces the potential for spurious correlations because it requires estimation of fewer vital rate parameters than a classical matrix model (Ellner and Rees 2006) and thus fewer vital rate correlations. The GLMM approach is the default statistical framework of stochastic integral projection models (Rees and Ellner 2009) but is similarly powerful in the context of stochastic matrix models, as demonstrated here and elsewhere (e.g., Evans et al. 2010). Finally, estimating correlations in a hierarchical Bayesian framework provides posterior probability distributions for correlation coefficients that reflect estimation uncertainty, which can then be propagated into the outputs of population projection models (Elderd and Miller 2016).

Once having estimated vital rate correlations, we then elucidate their role in stochastic population dynamics. The contributions of vital rates to stochastic population dynamics are typically unequal, because vital rates differ in both year-to-year variability (Pfister 1998) and sensitivity (e.g., Franco and Silvertown 2004). As a result, the strength of a correlation is not necessarily predictive of its effect on population growth (Doak et al. 2005). We used stochastic simulations to quantify the individual effects of pairwise vital rate correlations, as well as the combined effect of all correlations, on long-term fitness. In particular, we used simulations to quantify the contributions of vital rate correlations to the year-to-year variation in population growth rate (λ_t) and the long-term stochastic population growth rate (λ_s). For each of three perennial plant populations, we used long-term demographic data to address the following questions: (1) What are the sign, magnitude, and uncertainty of correlations between demographic vital rates? (2) What are the effects of specific pairwise vital rate correlations on the year-to-year variability of population growth? (3) Does the net effect of all vital rate correlations increase or decrease year-to-year variability in population growth? (4) What is the net effect of vital rate correlations on the long-term stochastic population growth rate (λ_s)?

Methods

Focal species and demographic data sets

We analyzed long-term demographic data from one population each of three species of iteroparous perennial plants: the aspen sunflower (*Helianthella quinquenervis*), the tree cholla cactus (*Opuntia* [=*Cylindropuntia*] *imbricata*), and the lady orchid (*Orchis purpurea*). *Helianthella quinquenervis* occurs in wet and boggy montane meadows of Western North America (Weber 1952). Our data came from a population at the Rocky Mountain Biological Laboratory in Colorado, USA (38°57′42.92″ N, 106°51′57.96″ W), where 3361 unique individuals were censused between 1998 and 2012 (details of data collection are provided in Appendix S1). *Opuntia imbricata* is a cactus found throughout the deserts and arid grasslands of Southwestern North America (Benson 1982). Our data came from a population at Sevilleta National Wildlife Refuge in central New Mexico, USA (34°20′5.3″ N, 106°37′53.2″ W), where 1001 unique individuals were censused between 2004 and 2015 (see Miller et al. [2009] and Ohm and Miller [2014] for details of study site and data collection). Finally, *Orchis purpurea* is an orchid that occurs in forest understories throughout the Mediterranean region of southern Europe (Rose 1948). Our data came from a population in eastern Belgium where 914 unique individuals were censused between 2003 and 2015 (see Jacquemyn et al. 2010, Miller et al. 2012). For all species, demographic data came from longitudinal studies in which individual plants were marked and censused annually for survival, size, and reproduction (number of flowers). In *H. quinquenervis*, size was

quantified by the number of rosette clumps (Inouye 2008). In *Op. imbricata*, the size variable was plant volume (cm³), based on height and width measurements (Miller et al. 2009). In *Or. purpurea*, the size variable was total leaf area (cm²), approximated using length and width measurements of individual leaves (Jacquemyn et al. 2010). For each species, we also had estimates of seedling recruitment as a function of previous seed production, allowing us to close the life cycle loop (Appendix S2).

Vital rate functions and correlations

The life histories of these perennial plants shared at least four main demographic vital rates for which we had data to model interannual variation and covariation: probability of survival, vegetative growth, probability of flowering, and fertility (number of flowers) of flowering plants, all of which we modeled as functions of plant size. For *H. quinquenervis* and *Or. purpurea*, we additionally modeled the temporal variation in the flower-to-fruit transition. In *H. quinquenervis*, temporal variation in this transition is strongly determined by the timing of spring snowmelt, which affects the floral abortion risk (Inouye 2008). In *Or. purpurea*, year-to-year fluctuations in pollinator limitation affect the probably that initiated flowers set fruit (Jacquemyn and Brys 2010). For *Op. imbricata*, we did not explicitly consider fruit set, which is very high due to efficient pollination services by specialist cactus bees (Ohm and Miller 2014). In addition, for *Or. purpurea* only, we modeled temporal variation in the probability of dormancy (this species can persist in a belowground dormant state). Thus, our study species had as few as four (*Op. imbricata*) and as many as six (*Or. purpurea*) time-varying vital rates. Interannual variability in these vital rates is presumably caused by climate fluctuations, though we did not explicitly model climate effects. Finally, for each species there was a set of unique vital rates, such as the number of seeds per fruit, the seed-to-seedling recruitment probability, and the probability of seed-banking, for which we had mean estimates but no information on temporal variance. Complete life cycle details for each species are provided in Appendix S2.

We modeled each of the time-varying vital rates by fitting generalized linear mixed-effect models to the long-term demographic data. Each vital rate was modeled as a linear function of plant size, with intercept α and slope β (except the flower-to-fruit transition, which had no size slope). We included temporal variation by allowing the intercepts to vary randomly from year to year (α_t), including the potential for correlated variation between vital rate intercepts. Preliminary analyses indicated that there was not enough information in the data to model temporal variation and co-variation in both the intercepts and slopes of the size-dependent vital rate functions. We therefore modeled temporal variation in the intercepts only, thus assuming that individuals of different size responded similarly to interannual variation.

Details of the vital rate models differed between species because size was a continuous variable in *Op. imbricata*

and *Or. purpurea* (volume and leaf area, respectively) but a discrete variable in *H. quinquenervis* (number of rosette clumps). To illustrate our approach to modeling vital rate correlations, we present here statistical models for the species with continuous size structure. In these species, growth was modeled with a normal distribution to populate a continuous kernel of size transitions, as in a classic integral projection model (IPM). Vital rate models for *H. quinquenervis* were very similar but growth was modeled with a negative binomial distribution, thereby populating a discrete projection matrix rather than a continuous kernel (Appendix S1). In the notation below, we use superscripted letters on intercepts (e.g., α^G) and slopes (β^G) to represent different vital rates ("G" for growth); note that these are not exponents. For growth, the response variable, $G_{i,t+1}$, was the $\log_e(\text{size})$ of individual i in year $t + 1$, which we modeled as normally distributed with time-independent standard deviation σ_G and mean given by a linear function of size in year t

$$G_{i,t+1} \sim \text{Normal}(\hat{G}_{t+1}, \sigma_G), \tag{1a}$$

$$\hat{G}_{t+1} = \alpha_t^G + \beta^G \log_e(\text{size}_t). \tag{1b}$$

For survival, the response $S_{i,t+1}$ described whether individual i was alive (success) or dead (failure) in year $t + 1$. Accordingly, we modeled survival as a Bernoulli process with probability of survival $\hat{S}_{t+1}$, which was given by a linear function of size in year t

$$S_{i,t+1} \sim \text{Bernoulli}(\hat{S}_{t+1}), \tag{2a}$$

$$\text{logit}(\hat{S}_{t+1}) = \alpha_t^S + \beta^S \log_e(\text{size}_t) \tag{2b}$$

where $\text{logit}(x)$ gives $\log(x/(1 - x))$. Like survival, the probability of flowering in year t was modeled as a Bernoulli process. The mean $\hat{P}_t$ of this Bernoulli process was given by a linear function of size in year t

$$P_{i,t} \sim \text{Bernoulli}(\hat{P}_t), \tag{3a}$$

$$\text{logit}(\hat{P}_t) = \alpha_t^P + \beta^P \log_e(\text{size}_t). \tag{3b}$$

Finally, for flowering plants, we modeled fertility as the number of reproductive structures. These were flowers in *Op. imbricata* and *Or. purpurea*, and flowering stems in *H. quinquenervis*, each of which produced multiple flowers (included in the model as a constant value; Appendix S2). The number of reproductive structures produced by individual i in year t, $F_{i,t}$, was modeled as a negative binomial process with overdispersion parameter Θ_F, and mean $\hat{F}_t$ given by a linear function of size in year t

$$F_{i,t} \sim \text{NB}(\hat{F}_t, \Theta_F), \tag{4a}$$

$$\log(\hat{F}_t) = \alpha_t^F + \beta^F \log_e(\text{size}_t). \tag{4b}$$

In *Or. purpurea* and *H. quinquenervis*, we also modeled an additional time-varying vital rate: the flower-to-fruit transition probability. We modeled this vital rate as a beta-binomial process. We used an alternative parameterization of the beta-binomial distribution that is based on a mean probability of successes (fruits), $\hat{M}_t$, the number of trials, represented by the number of reproductive structures $F_{i,t}$, and an overdispersion parameter Θ_M (Morris 1997):

$$M_{i,t} \sim \text{BetaB}(\hat{M}_t, F_{i,t}, \Theta_M), \tag{5a}$$

$$\text{logit}(\hat{M}_t) = \alpha_t^M. \tag{5b}$$

Last, in *Or. purpurea* only, we modeled the probability of dormancy in year $t + 1$ as a Bernoulli process with mean probability given by a linear function of size in year t

$$D_{i,t+1} \sim \text{Bernoulli}(\hat{D}_{t+1}), \tag{6a}$$

$$\text{logit}(\hat{D}_{t+1}) = \alpha_t^D + \beta^D \log_e(\text{size}_t). \tag{6b}$$

The time-varying vital rates were linked via the intercepts of the size-dependent functions, which were drawn from a multivariate normal (MVN) distribution with mean vector $\boldsymbol{\mu}$ and variance-covariance matrix $\boldsymbol{\Sigma}$. For example, for *Op. imbricata*, whose model included four time-varying vital rates,

$$\boldsymbol{\alpha}_t = \begin{bmatrix} \alpha^G \\ \alpha^S \\ \alpha^P \\ \alpha^F \end{bmatrix}_t, \tag{7a}$$

$$\boldsymbol{\alpha}_t \sim \text{MVN}(\boldsymbol{\mu}, \boldsymbol{\Sigma}), \tag{7b}$$

$$\boldsymbol{\mu} = \begin{bmatrix} \mu^G \\ \mu^S \\ \mu^P \\ \mu^F \end{bmatrix}, \tag{7c}$$

$$\boldsymbol{\Sigma} = \begin{bmatrix} \sigma^G \sigma^G & \sigma^S \sigma^G \rho_{SG} & \sigma^P \sigma^G \rho_{PG} & \sigma^F \sigma^G \rho_{FG} \\ \sigma^G \sigma^S \rho_{GS} & \sigma^S \sigma^S & \sigma^P \sigma^S \rho_{PS} & \sigma^F \sigma^S \rho_{FS} \\ \sigma^G \sigma^P \rho_{GP} & \sigma^S \sigma^P \rho_{SP} & \sigma^P \sigma^P & \sigma^F \sigma^P \rho_{FP} \\ \sigma^G \sigma^F \rho_{GF} & \sigma^S \sigma^F \rho_{SF} & \sigma^P \sigma^F \rho_{PF} & \sigma^F \sigma^F \end{bmatrix} \tag{7d}$$

The symmetric matrix $\boldsymbol{\Sigma}$ includes the vital rate variances (expressed as products of the standard deviations) on the diagonal and covariances (expressed as products of the standard deviations and correlation coefficients) on the sub-diagonal. We used a similar approach for *H. quinquenervis* and *Or. purpurea*, but these species had, respectively, one and two additional time-varying vital rates and therefore dimension 5×5 and 6×6.

Parameter estimation

We estimated the parameters of the vital rate functions, including the vital rate correlations ρ_{ij}, in a hierarchical Bayesian framework. This approach allowed us to model all time-varying vital rates in a single analysis rather than piece by piece; this means that we could simultaneously estimate vital rate parameters and their

temporal variances and covariances. In addition, the output of a Bayesian analysis is a posterior probability distribution for each parameter mean, variance, and covariance, reflecting the uncertainty in the estimates given the uncertainty in the data. These posterior distributions allow us to transfer the uncertainty in vital rate estimation to the uncertainty in the output of the population models.

We fit our models in Stan (Stan Development Team 2015), a programming language that allows Bayesian inference without requiring conjugacy of priors. The central objective of our statistical models was to estimate the correlations and variances of vital rates (the lower-level parameters of Σ) separately. In stochastic population dynamics, the variance of vital rates and the correlation among vital rates have distinct effects (Doak et al. 2005). In previous studies, ecologists have estimated Σ using an inverse Wishart prior (e.g., Ibáñez et al. 2009). This is the only known conjugate prior for Σ and is thus an obligate choice for the most popular packages that fit Bayesian models using Gibbs sampling (e.g., Lunn et al. 2000, Plummer 2003). However, using an inverse Wishart prior for Σ produces biased estimates whereby correlations and variances are not independent (Gelman and Hill 2007). We therefore used Stan, which fits models using No-U-Turn (Hoffman and Gelman 2014) or Hamiltonian Monte Carlo (Duane et al. 1987) sampling, a powerful alternative that allowed us to estimate variances and correlations independently.

We fit the Bayesian models using uninformative priors for all parameters. We decomposed the variance–covariance matrix to $\Sigma = \mathrm{diag}(\boldsymbol{\sigma})\,\mathbf{P}\,\mathrm{diag}(\boldsymbol{\sigma})$, where diag() returns a diagonal matrix, $\mathbf{P}$ is a matrix of pairwise correlation coefficients, and $\boldsymbol{\sigma}$ is a vector that contains the standard deviations. We estimated the correlation matrix $\mathbf{P}$ using an LKJ prior (the acronym refers to the initials of the authors in Lewandowski et al. 2009), and the standard deviation of each vital rate intercept ($\sigma^S, \sigma^G, \sigma^P, \sigma^F, \sigma^M, \sigma^D$) using Cauchy priors. We used normal priors for the α and β regression coefficients (Eqs. 1–6), and an inverse gamma prior for σ_G (Eq. 1a). Moreover, we used uniform priors with support [0, 100] for the negative binomial overdispersion parameters Θ_G (Eq. S.1a) and Θ_F (Eq. 4a), and a Pareto prior for the beta binomial overdispersion parameter Θ_M (Eq. 5a, Gelman et al. 2013). We fit models using the RStan package (Stan Development Team 2015). We ran four 5000-iteration Markov chain Monte Carlo simulations, discarding the initial 1000 iterations. This number of iterations is usually sufficient for model convergence when taking Hamiltonian Monte Carlo samples, and was sufficient to reach convergence in *H. quinquenervis* and *Op. imbricata* according to Brooks and Gelman's (1998) potential scale reduction factor ($\hat{r}$). In *Or. purpurea*, models converged after 30000 iterations. We evaluated model fit by carrying out posterior predictive checks (Appendix S3: Figs. S1–S3) and by visualizing predictions of the models against raw data (Appendix S2). For each parameter, we estimate its 95%

credible interval (the inner 95% density of the posterior distribution).

Population modeling

We used the vital rate model parameters, including the vital rate correlations, to build stochastic population projection models. We built IPMs for *Op. imbricata* and *Or. purpurea*, and a matrix population model (MPM) for *H. quinquenervis*. Both IPMs and MPM describe the dynamics of populations structured by one or more state variables. Here, our state variable was the size of individuals, such that IPMs were appropriate for continuous size (*Op. imbricata* and *Or. purpurea*) and a MPM was appropriate for discrete size (*H. quinquenervis*). In our models, the discrete time step (t to $t + 1$) corresponded to one year. For the IPMs, the continuous state variable was $\log_e$(size) and size structure dynamics were projected as

$$n(y)_{t+1} = \int_L^U K(y,x;\boldsymbol{\alpha}_t)n(x)_t\,dx. \qquad (8)$$

The kernel function $K(y,x;\boldsymbol{\alpha}_t)$ is a surface that describes all possible transitions from $\log_e$(size) x at time t to $\log_e$(size) y at time $t + 1$. The vector $\boldsymbol{\alpha}_t$ is the vector of time-varying parameters that govern temporal variability in the kernel (Eq. 7). L and U are, respectively, the lower and upper limits of the $\log_e$(size) distribution.

For the *H. quinquenervis* MPM, population dynamics were projected according to

$$\mathbf{n}_{t+1} = \mathbf{A}(\boldsymbol{\alpha}_t)\mathbf{n}_t. \qquad (9)$$

Here, $\mathbf{n}$ is a vector that includes the abundance of each discrete size (clump number) and $\mathbf{A}(\boldsymbol{\alpha}_t)$ is a projection matrix that describes all possible transitions from size x to size y. Similarly to the IPM kernel (Eq. 8), the projection matrix takes the vector of year-specific vital rates, $\boldsymbol{\alpha}_t$, which governs its temporal variability. Eqs. 8 and 9 are a generic representation of our stochastic population projection models: in Appendix S2 we provide detailed, species-specific versions of Eqs. 8 and 9, which also include discrete states of the life cycle such as below-ground tubers and dormant plants in *Or. purpurea* and seed banks in *Op. imbricata*.

We ran stochastic simulations of the IPMs and MPM using fitted estimates for the vital rate means, variances, and covariances (presented in Appendix S2). These simulations provided baseline estimates for the variability of the year-specific geometric population growth rates ($\mathrm{Var}(\lambda_t)$) and the stochastic long-term population growth rate (λ_s). For the simulations, we defined a stochastic sequence of environments by drawing 50000 vectors (years) for $\boldsymbol{\alpha}_t$ according to a multivariate normal distribution based on empirical estimates for mean vector $\boldsymbol{\mu}$ and variance–covariance matrix Σ, following Eq. 7a–d. We then simulated the population models 50000 times and analyzed data from the last 45000 time steps, excluding the initial transient dynamics of the size

distribution. We first simulated population dynamics using the mean values of vital rate parameters' joint posterior. To quantify uncertainty in our inferences for $\text{Var}(\lambda_t)$ and λ_s, we replicated simulations by running 100 separate population projection models built using 100 random samples from the joint posterior distribution of all vital rate parameters, including those associated with stochasticity: the coefficients of the correlation matrix $\mathbf{P}$ and the vector of standard deviations $\boldsymbol{\sigma}$. We considered 100 a sensible number of posterior draws, because as few as 25 draws provided a qualitatively similar range of estimate uncertainty as our final results (Appendix S4).

Effects of vital rate correlations on the variance of population growth

We first asked how individual vital rate correlations and the combination of all pairwise correlations modified the variance of year-to-year population growth rates, motivated by the predictions that negative and positive correlations should tend to decease and increase $\text{Var}(\lambda_t)$. To do this, we ran models projecting populations whose vital rates varied independently (correlations "off") and contrasted the results with the baseline simulations described above (correlations "on"), holding all else equal between the two treatments, including the same random sequence of temporal variation. For the no-correlation models, we modified $\mathbf{P}$ matrices to simulate populations where (1) only one pairwise correlation was turned off and (2) all vital rate correlations were turned off. These two approaches provide complementary information, since a weak combined effect of all correlations could reflect uniformly weak effects of individual correlations or strong opposing effects of pairwise correlations that cancel each other out. For the analysis of individual correlations, we set two elements of the $\mathbf{P}$ matrix equal to 0, such that $\rho_{ij} = \rho_{ji} = 0$. We repeated this process for each pairwise vital rate correlation. For the analysis of all correlations combined, all non-diagonal elements of the $\mathbf{P}$ matrix were set equal to 0, so that $\mathbf{P}$ was an identity matrix $\mathbf{I}$, and the variance–covariance matrix was given by $\boldsymbol{\Sigma} = \text{diag}(\boldsymbol{\sigma})\,\mathbf{I}\,\text{diag}(\boldsymbol{\sigma})$. The difference in $\text{Var}(\lambda_t)$ between simulations with correlations on and off estimates the effect of vital rate correlation on $\text{Var}(\lambda_t)$. To compare results across species, we calculated the percentage change in variance relative to the case with correlations off ($\Delta\text{Var}(\lambda_t) = 100 \times [\text{Var}(\lambda_{t,\text{on}}) - \text{Var}(\lambda_{t,\text{off}})]/\text{Var}(\lambda_{t,\text{off}})$). Finally, to account for uncertainty, we replicated these simulation experiments for each of 100 draws from the joint posterior distribution of all vital rate parameters.

We also used an alternative, analytical approach to quantify the effect of vital rate correlations on the temporal variance of population growth by performing a life table response experiment (LTRE). Rees and Ellner (2009) provide an LTRE approximation that decomposes year-to-year variability in population growth into contributions from the variances and covariances of all vital rates, weighted by their sensitivities. Importantly,

this LTRE method approximates only the variance of the asymptotic population growth rate associated with each year (i.e., the leading eigenvalue of each year-specific kernel or matrix, $\lambda_{1,t}$). The realized growth rates (λ_t) deviate from these asymptotic values due to fluctuations in the population size structure, which does not reach a stable distribution in a stochastic environment. The variance of $\lambda_{1,t}$ is a relevant but incomplete measure of stochastic population dynamics because at each time step $\lambda_t = \lambda_{1,t} \times$ reactivity$_t$ (Ellis and Crone 2013, McDonald et al. 2016). Here, $\lambda_{1,t}$ represents the long-term effect of vital rates, while reactivity$_t$ measures the transient response of a population, whereby reactivity$_t \neq 1$ when a population is not at its stable stage distribution (Neubert and Caswell 1997). We are not aware of an LTRE approximation for the actual realized growth rates λ_t, which is why we focus on the simulation approach. We present the LTRE decomposition of $\text{Var}(\lambda_{1,t})$ in Appendix S5 (including additional methods) as a complement to our simulation results, because this captures the influence of demographic correlations in isolation from stochastic fluctuations in population structure, which can be a substantial source of variability in population growth (Ellis and Crone 2013, McDonald et al. 2016).

The effect of vital rate correlations on the long-term stochastic population growth rate (λ_s)

We estimated the effect of vital rate correlations on the long-term stochastic population growth rate (λ_s), motivated by the predictions that negative and positive correlations should tend to have positive and negative effects, respectively, on λ_s via their influence on $\text{Var}(\lambda_t)$. The long-term stochastic population growth rate is given by the geometric mean of a long series of yearly population growth rates

$$\log(\lambda_S) = E\left[\log\left(\frac{N_{t+1}}{N_t}\right)\right]$$

where N is total population size summed across sizes and stages (Caswell 2001, Rees and Ellner 2009). This series was provided by the last 45000 values of year-to-year population growth rates (λ_t) from our simulations. As above, we compared λ_s between simulation treatments with all vital rate correlations on ($\lambda_{s,\text{on}}$) or off ($\lambda_{s,\text{off}}$). That is, vital rates either covaried according to empirical estimates ($\boldsymbol{\Sigma} = \text{diag}(\boldsymbol{\sigma})\,\mathbf{P}\,\text{diag}(\boldsymbol{\sigma})$) or varied independently ($\boldsymbol{\Sigma} = \text{diag}(\boldsymbol{\sigma})\,\mathbf{I}\,\text{diag}(\boldsymbol{\sigma})$). To estimate the long-term fitness effect of vital rate correlations, we calculated the percent difference between these two simulation treatments, so that $\Delta\lambda_s = 100 \times [\lambda_{s,\text{on}} - \lambda_{s,\text{off}}]/\lambda_{s,\text{off}}$. If vital rate correlations buffer population growth against negative effects of variability, $\Delta\lambda_s$ is positive; if correlations amplify the negative effects of variability, $\Delta\lambda_s$ is negative. Note that in these simulations, temporal variances $\boldsymbol{\sigma}$ were constant across the two treatments, thus isolating demographic correlations *per se* from demographic variability. We created a posterior distribution of $\Delta\lambda_s$ using 100 samples

from the joint posterior distribution of the vital rate parameters. The distributions of $\Delta\lambda_s$ values therefore reflect all of the uncertainty in our estimates of vital rate coefficients, including uncertainty in estimates of temporal variances and correlations.

<div style="text-align:center">RESULTS</div>

(1) What are the sign, magnitude, and uncertainty of correlations between demographic vital rates?

Vital rate correlations varied greatly in both sign and magnitude, and uncertainty in their estimates was high (Fig. 1). Across all species and vital rates, there were only two correlations for which the posterior probability distribution indicated an unambiguous sign (their 95% credible interval excluded zero): the positive correlation between the probability of flowering and fertility in *H. quinquenervis* (mean ρ = 0.82; 95% CI = [0.51; 0.96]) and the negative correlation between growth and fertility in *Or. purpurea* (mean ρ = -0.53; 95% CI = [−0.85; −0.05]). There were two additional correlations for which a majority of the posterior distribution indicated a

consistent sign (but the 95% CI included zero): the positive correlation between the probability of flowering and fertility in *Or. purpurea* (mean ρ = 0.45; 95% CI = [−0.06; 0.80]) and the negative correlation between growth and flower-to-fruit transition probability in *H. quinquenervis* (mean ρ = -0.43; 95% CI = [−0.77; 0.03]). For the cactus *Op. imbricata*, there were no correlations for which the posterior distribution indicated a clear sign and most posterior modes were weak in magnitude. The positive correlations between flowering and fertility in *H. quinquenervis* and *Or. purpurea* indicate that years in which flowering was more likely were also years of greater seed production by flowering plants; this correlation was also positive, on average, for *Op. imbricata*, though there was greater uncertainty in its estimate (Fig. 1). On the other hand, the negative correlations indicate that years of greater reproductive effort or success were associated with smaller gains in size, and vice versa. In *Or. purpurea*, the negative correlation occurred between growth and the number of flowers produced, regardless of whether the flowers set fruit. In *H. quinquenervis*, the negative correlation occurred between growth and floral abortion (high floral abortion [i.e., low flower-to-fruit transition]
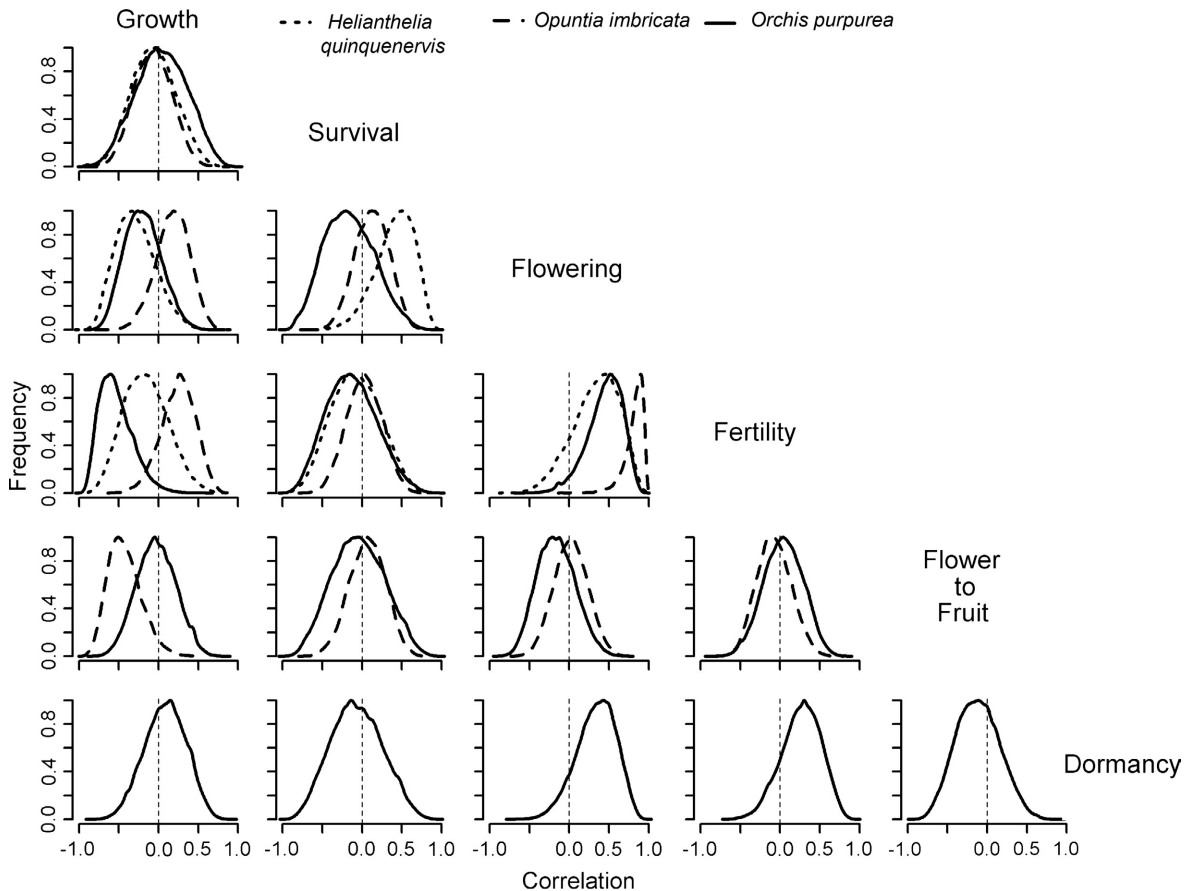

FIG. 1. Posterior probability distributions of vital rate correlations. Each panel represents a vital rate pair. Line types represent species.

was associated with high growth, and vice versa). The remaining correlations, which were most of the correlations, did not have a predominant sign within or across species, and their mean magnitude was usually small (Fig. 1).

The uncertainty of vital rate correlations was large compared to the uncertainty of other parameters (Appendix S2: Tables S1–S3). Because correlation estimates are constrained between −1 and 1, the standard deviation of their posterior is constrained as well. On the other hand, most other parameters can vary between −∞ and ∞, or between 0 and ∞ (Appendix S2), so that the standard deviation of their posterior is unconstrained. Nevertheless, the standard deviation of these other parameters was similar to or smaller than the standard deviation of correlation estimates, suggesting relatively greater uncertainty in the correlations.

Time series for the intercepts of vital rate models (standardized to mean zero and unit variance, for visual comparison) demonstrate how vital rate correlations played out across years (Fig. 2). Using *H. quinquenervis* as an example (Fig. 2A), the intercepts for fertility and the probability of flowering are almost completely overlapping, reflecting their strong positive correlation (Fig. 1). For example, in 2002, few plants initiated flowering stalks and those that did produced few inflorescences. On the other hand, the intercepts for growth and the flower-to-fruit transition vary in opposite directions, reflecting their negative temporal correlation. For example, 2003 and 2004 were the two worst years for flower viability and the two best years for growth, and 1999 and 2008 were the opposite. Similarly, in *Or. purpurea* (Fig. 2C), 2007 was a year of unusually low fertility and unusually high growth, and 2011 and 2013 were the opposite. In *Op. imbricata* (Fig. 2B), 2011 was an exceptionally bad year for most vital rates, following an unprecedented four-day deep-freeze that brought record

low temperatures. However, this strong forcing event was not sufficient to drive strong positive correlations because vital rate fluctuations were independent across the other, more benign years of the study.

(2) What are the effects of specific pairwise vital rate correlations on the year-to-year variability of population growth?

The proportional change in variance of year-to-year population growth rates ($Var(\lambda_t)$) caused by pairwise vital rate correlations varied idiosyncratically across species but was generally weak and centered near zero (Fig. 3). In fact, there was not one pairwise correlation, across all three species, whose effects on population growth variability were unambiguous in sign based on the posterior probability distribution. The directional effects of correlations were generally consistent with expectations, where negative correlations tended to reduce variability and positive correlations tended to increase it. For example, the strong positive correlation between flowering and fertility in *H. quinquenervis* tended to increase variability. However, the contributions of vital rate correlations to population growth variability did not necessarily correspond well to the magnitude of the correlations. This reflects the fact that the effect of a correlation depends on both its absolute magnitude and the sensitivities of population growth to the two vital rates involved, highlighting the importance of vital rate sensitivities and their absolute temporal variability in addition to correlations (Appendix S5: Eq. S.3a,b, Table S1). For example, in *H. quinquenervis*, the negative correlation between growth and flower-to-fruit transition ($\rho = -0.43$) decreased $Var(\lambda_t)$ by just 3% on average. Similarly, in the other two species, the largest effects on $Var(\lambda_t)$ did not correspond to the strongest correlations. Results from *Or. purpurea* were particularly surprising in

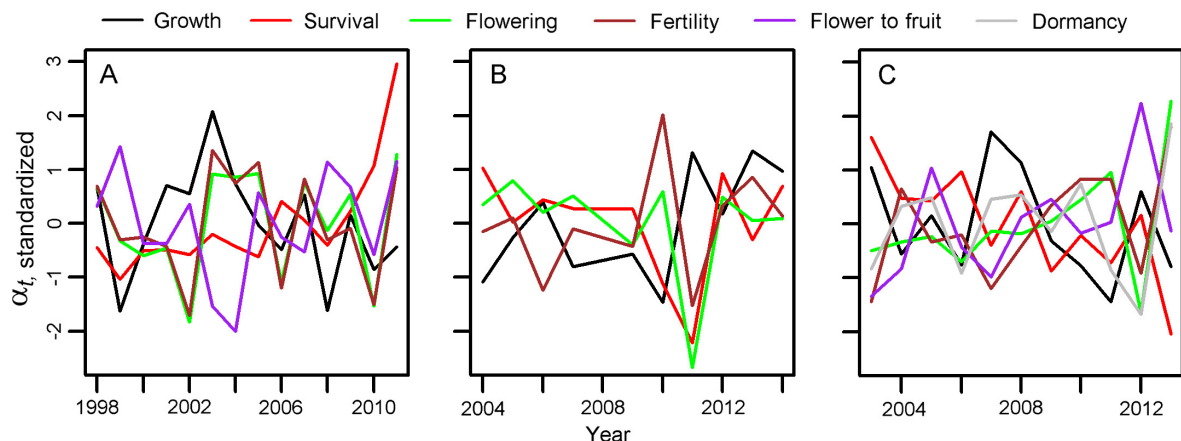
Fig. 2. Year-specific intercepts of vital rate models (e.g., Eq. 7). Line colors represent different vital rates. Panels show results for *Helianthelia quinquenervis* (A), *Opuntia imbricata* (B), and *Orchis purpurea* (C). For each species, we standardized the intercept α_t^{VR} for each vital rate VR so that $\alpha_{t,standardized}^{VR} = (\alpha_t^{VR} - \alpha_{mean}^{VR})/\alpha_{sd}^{VR}$.
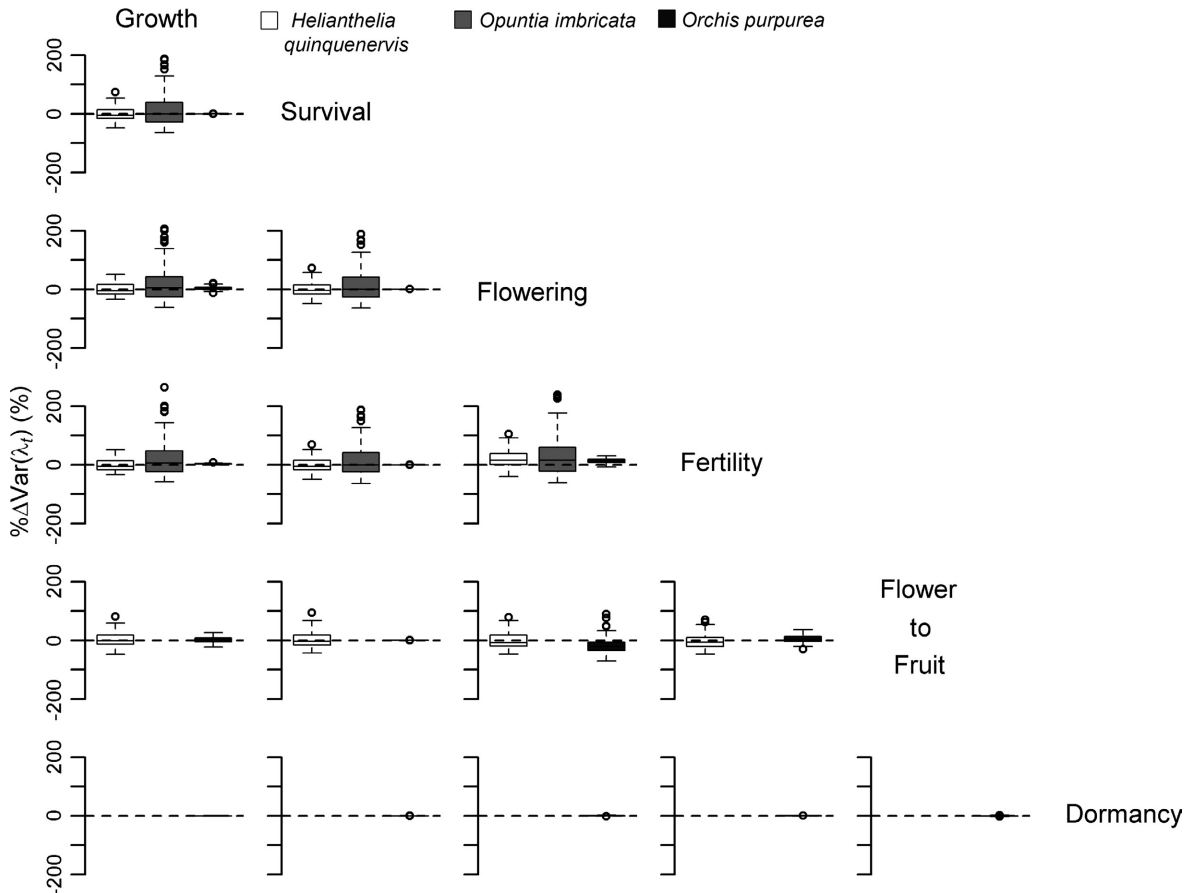
FIG. 3. Change in the variance (ΔVar) of year-to-year population growth rates (λ_t) caused by pairwise vital rate correlations. We present the percent difference between simulations accounting for vital rate correlations ("on") and simulations where vital rates varied independently ("off"). Each panel represents the percent change in variance caused by the correlation of a specific vital rate pair. This percent change is $100 \times [\text{Var}(\lambda_{t,\text{on}}) - \text{Var}(\lambda_{t,\text{off}})]/\text{Var}(\lambda_{t,\text{off}})$. Gray levels represent species. Box-and-whisker plots represent values produced by simulations run using 100 random samples from the joint posterior distribution of model parameters. Lines in the middle of each box are medians, box limits show the first and third quartile, whiskers extend beyond box limits 1.5 times the interquartile range, and open points are outliers.

that most vital rate correlations had little effect on Var(λ_t). Moreover, the strongest mean contribution to Var(λ_t) (-18%) is made by a relatively weak correlation between flowering and flower-to-fruit transition ($\rho = -0.16$; Fig. 1). Finally, the posterior distributions of the change in Var(λ_t) were extremely wide, especially in *H. quinquenervis* and *Op. imbricata*, reflecting uncertainty in our estimates of the vital rates and their variances and correlations. These posterior distributions always included zero, and the uncertainty intervals ranged from -70% to $+260\%$.

(3) Does the net effect of all vital rate correlations increase or decrease year-to-year variability in population growth?

On average, the net effect of all combined vital rate correlations increased the year-to-year variability of population growth in *H. quinquenervis* and *Op. imbricata*, and

caused no change in variability for *Or. purpurea* (Fig. 4A). Yet, uncertainty in these effects was high, posterior belief was distributed across both positive and negative values, and all credible intervals included zero. According to the simulations based on the mean of the joint posterior of parameter estimates (dots in Fig. 4A), in *H. quinquenervis* and *Op. imbricata* the variance-amplifying effects of positive correlations generally outweighed the variance-reducing effects of negative correlations, but correlations had virtually no effect on variance in *Or. purpurea*. In particular, vital rate correlations changed the variability of population growth, on average, by $+20.8\%$ in *H. quinquenervis*, $+22.51\%$ in *Op. imbricata*, and -1% in *Or. purpurea*. However, the credible intervals of posterior estimates were extremely wide, with a range of values that span from -71% to $+157\%$.

In contrast to the simulation experiments, the LTRE decomposition of variability (Var($\lambda_{1,t}$)), excluding the influence of non-equilibrium size structure dynamics,
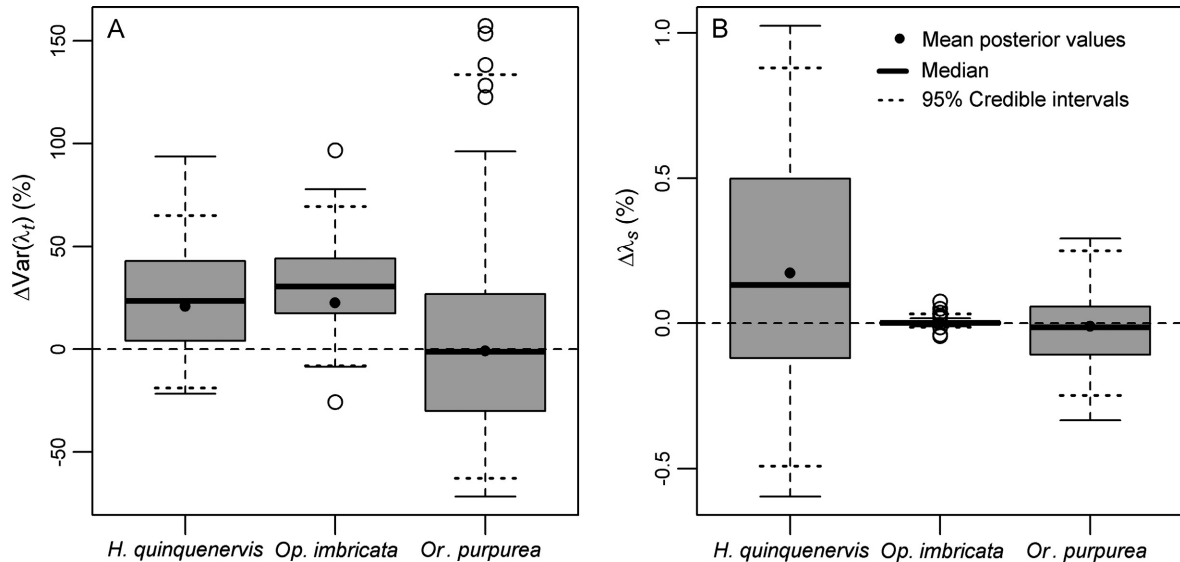
Fig. 4.   The effect of vital rate correlations on the variance of year-to-year population growth rate (λ_t, panel A), and on long-term stochastic population growth rate (λ_s, panel B). We present percent changes in both quantities. In panel A, $\Delta Var(\lambda_t)$ is calculated as in Fig. 3. Similarly, in panel B, $\Delta\lambda_s$ is $100 \times [\lambda_{s,on} - \lambda_{s,off}]/\lambda_{s,off}$. Black dots refer to simulations results from population models built using the mean values of the parameters' joint posterior. Box-and-whisker plots show the values calculated using 100 random samples from the joint posterior distribution of vital rate parameters. Box limits, whiskers, and open dots are as in Fig. 3. Dotted lines delimit the upper and lower bounds of the 95% credible intervals of posterior values.

suggested that, for all three species, vital rate correlations should consistently buffer the variability of growth rates, on average (Appendix S5: Fig. S1). LTREs showed an average decrease in $Var(\lambda_{1,t})$ for *H. quinquenervis* (−8.59%), *Op. imbricata* (−4.26%), and *Or. purpurea* (−17.37%). However, just like the estimates from simulation experiments, the uncertainty associated with the LTRE estimates was large: posterior probabilities were distributed across positive and negative effects of correlations, and credible intervals included zero (Appendix S5: Fig. S1).

(4) What is the net effect of vital rate correlations on the long-term stochastic population growth rate (λ_s)?

Across all three species, the effect of vital rate correlations on long-term stochastic population growth rate (λ_s) was small in magnitude and virtually zero, on average (Fig. 4B). The credible intervals of λ_s show very small effects that range from −0.49% to +0.88% in *H. quinquenervis*, from −0.01% to +0.03% in *Op. imbricata*, and from −0.25% to 0.25% in *Or. purpurea*. On average, vital rate correlations changed the stochastic population growth rate by +0.17% in *H. quinquenervis*, +0.002% in *Op. imbricata*, and −0.01% in *Or. purpurea*.

Posterior distributions for the absolute values of λ_s are shown in Appendix S6. Results indicated that the *Op. imbricata* population is almost certainly declining, because no posterior sample produced λ_s values greater than 1.0 (95% CI = [0.93; 0.99]). *H. quinquenervis* is also projected to decline, though the uncertainty in its

stochastic population growth rate included the possibility of positive growth (95% CI = [0.91; 1.04]). On the other hand, the posterior distribution of λ_s in *Or. purpurea* exceeded 1.0, so this population is expected to grow (95% CI = [1.05; 1.10]). All of these predictions for population viability were insensitive to whether demographic correlations were on or off (Appendix S6). Thus, qualitatively and even quantitatively, explicit accounting of vital rate correlations did not change our understanding of the dynamics and viability of these populations.

DISCUSSION

Natural populations encounter stochastic fluctuations in demographic vital rates from year to year. Theory predicts a potentially important role for correlated vital rate fluctuations in long-term population viability (Tuljapurkar 1982, Doak et al. 2005). Yet, empirical understanding of whether vital rate correlations are sufficiently common and of sufficient magnitude to meaningfully affect population dynamics has lagged behind theory. Our work provides new insight into the occurrence and consequences of vital rate correlations in natural populations, revealing both consistencies and idiosyncrasies across long-term data sets from three perennial plant species. Our most important conclusion is that, while a few strong vital rate correlations were detected from long-term data, overall, correlations had virtually no influence on the stochastic population growth rate or on inferences regarding population viability. Thus, if results from these three study populations are

broadly representative, the non-trivial task of quanti-fying correlations and incorporating them into demo-graphic models may often be unnecessary for drawing qualitative and even quantitative inferences regarding population dynamics in stochastic environments.

Correlations may be positive or negative, with the sign reflecting different biological mechanisms. Our study suggests certain correlations may be influenced by trade-offs between vegetative growth and reproductive function. This is suggested by the negative correlations between growth and fertility in *Or. purpurea*, and between growth and flower-to-fruit transition in *H. quinquenervis*. While negative correlations do not necessarily represent life history trade-offs (Knops et al. 2007), detailed studies of *Or. purpurea* (Jacquemyn et al. 2010, Miller et al. 2012) provide evidence for a cost of reproduction at the level of individual plants consistent with our current findings. Trade-offs between reproductive and somatic life history functions, usually documented at the individual level, are common in plants (e.g., Harper 1977, Woodward et al. 1994, Silvertown and Dodd 1999, Obeso 2002). Our results suggest that these trade-offs can generate negative temporal vital rate correlations in plant populations, such that years of high reproductive effort or success are years of poor growth, and vice versa (Fig. 2). However, the remaining vital rate correlations were generally weak and varied idiosyncratically within and across species.

The lack of consistent pattern in the direction and mag-nitude of vital rate correlations is supported by some lit-erature on plants (Evans et al. 2010, Jacquemyn et al. 2012, Davison et al. 2013) and animals (Doak et al. 1994, Reed and Slade 2006a, b). For example, several studies that linked climatic fluctuations to plant demography did not find common responses of vital rates to climate drivers (Clark et al. 2011, Dalgleish et al. 2011, Adler et al. 2012, Williams et al. 2015), suggesting that vital rates respond individualistically to climatic variability. On the other hand, two comparative studies that focused on animals reported predominantly positive temporal correlations between vital rates (Saether and Bakke 2000, Morris et al. 2011). However, most of the positive corre-lations reported in these matrix modeling studies occurred between the survival of different size classes: for example between survival of juveniles and adults. These positive correlations across size classes are implicit in our popu-lation projection models because they are built into the random intercepts of GLMMs. In our GLMMs, a "good" year for survival is assumed to be good across all sizes, which makes our estimation of correlations more conservative than these previous studies.

Our estimation process revealed substantial uncer-tainty, particularly for correlations whose posterior mode was small in magnitude, where posterior weight was distributed across positive and negative values (Fig. 1). The uncertainty in the estimates of correlation was larger than the uncertainty of most other parameter estimates (Tables S1–S3). Such high uncertainty indicates that even one decade of data provide low power when

estimating correlations among vital rates. This is perhaps not surprising: the sample size necessary to precisely estimate a correlation of 0.1 is ~250 (Schönbrodt and Perugini 2013), far longer than any complete demo-graphic data set that we know of. Thus, even our unu-sually long-term studies may not have provided enough information to unambiguously detect real but weak cor-relations, highlighting the importance of explicitly accounting for uncertainty. Rather than dismiss weak correlations outright, our Bayesian approach exploited the full posterior distributions of all vital rate correla-tions, even those centered near zero. This approach pro-vides a probabilistic assessment of how correlations affect stochastic population dynamics, given our confi-dence in the estimation process. We expect that uncer-tainty in the correlation coefficients, particularly the weak ones, will become better resolved as these ongoing demographic studies continue and more data accumulate. Nevertheless, given that most of the correlation estimates and their effects on stochastic population growth were centered at or near zero, we expect our conclusions to stand, even with better resolved correlations. Importantly, despite the uncertainty in estimation of the vital rate cor-relations, we are quite certain that their effects on the stochastic growth rate are negligible, given the posterior distributions of $\Delta\lambda_s$ (Fig. 4B).

Our simulations suggested that vital rate correlations could have potential to modify long-term population growth because their combined effect, on average, increased the variability of year-to-year population growth (Var(λ_t)) in two species (Fig. 4A). For these species, positive correlations apparently outweighed neg-ative correlations, causing on average an increase in var-iability, though the uncertainty in correlations contributed to wide posterior distributions for their effects on var-iance. Taken in isolation, these results could be inter-preted to reinforce the importance of vital rate correlations as modifiers of demographic variability (Tuljapurkar 1982, Boyce et al. 2006, Tuljapurkar et al. 2009). However, our simulations of stochastic population dynamics revealed consistently that vital rate correlations had vir-tually no effects (<1% change) on the stochastic growth rate, λ_s (Fig. 4B); this was true for *Or. purpurea*, where correlation caused, on average, no change in Var(λ_t) but also, more surprisingly, in *H. quinquinervis* and *Op. imbricata*, where correlations caused a mean increase in Var(λ_t) of 21% and 23%, respectively. This apparent discrepancy is likely explained by the fact that a large proportional effect of correlations on year-to-year varia-bility need not translate into a large effect on λ_s. We pre-sented percent changes in Var(λ_t) and λ_s in order to directly compare results across species. However, the stochastic population growth rate is sensitive to absolute rather than relative changes in Var(λ_t) (Lewontin and Cohen 1969). If absolute variability is already small then an increase of 10–20% may have negligible effects on λ_s. For example, Morris et al. (2011) attributed very weak effects of vital rate covariation and temporal

autocorrelation on stochastic population growth of primates, effects comparable in magnitude to our results from perennial plants, to low baseline demographic variability. We speculate that vital rate correlations may generally have negligible effects for populations already buffered against temporal variability, as long-lived organisms tend to be (Morris et al. 2008).

Another surprising result from our simulations was the direction of correlation effects on year-to-year variability (Fig. 4A) relative to the direction of effects on λ_s (Fig. 4B). While none of these effects were strong, the mean increase of $\mathrm{Var}(\lambda_t)$ in *H. quinquinervis* and *Op. imbricata* was not associated with a mean decrease in λ_s, as would be predicted by classic theory. We speculate that this result may have been caused by the canonical link functions that we used to model temporal variability in vital rates (e.g., Eqs. 2b, 3b, 4b). These link functions are standard tools for the development of stochastic IPMs (Rees and Ellner 2009) but they introduce some nonlinear averaging. Canonical link functions implicitly assume that demographic processes respond nonlinearly to random variation. As a consequence, nonlinear averaging might arise whereby the value of a vital rate in an average year is greater or less than the value of the vital rate averaged across years. The magnitude of this difference depends on the magnitude of year-to-year variability and on the concavity of the link function (Ruel and Ayres 1999). For instance, the log-link function we used in our fertility models (Eq. 4b) is concave up. As a result, an increase in temporal variation could potentially increase average fertility and, potentially, stochastic population growth rate (Barraquand and Yoccoz 2013). A deeper analysis of this issue falls outside the scope of our study, but we suggest that it warrants greater attention in the methodological literature on stochastic demography. Given the small magnitudes of the effects we detected (Fig. 4B) any contributions of nonlinear averaging in our study are unlikely to affect our qualitative conclusions.

Our λ_s results suggest that vital rate correlations should have negligible evolutionary implications in our three species. Vital rate correlations are expected to modulate the evolution of demographic buffering, whereby selection decreases the temporal variance of vital rates (Pfister 1998, Morris and Doak 2004). In particular, positively correlated vital rates, by increasing $\mathrm{Var}(\lambda_t)$ and decreasing λ_s, should promote selection for lower temporal variance in vital rates; vice-versa for negatively correlated vital rates (Doak et al. 2005). However, because in our three species vital rate correlations have negligible effects on λ_s, such correlations should have a similarly minor effect on the evolution of demographic buffering.

Lastly, the contrast between our simulation experiments (Fig. 4A) and LTRE analyses (Appendix S5: Fig. S1) highlights a role for stochastic fluctuations in size structure as a potentially important component of demographic variability, as has been recently emphasized (Ellis and Crone 2013, McDonald et al. 2016). The LTRE approach used year-specific asymptotic population growth rates, $\lambda_{1,t}$, as a proxy for the realized year-to-year population growth rate, λ_t. However, the constant fluctuations in size structure that are characteristic of populations in stochastic environments may cause realized growth rates (λ_t) to deviate from expectations based solely on vital rates ($\lambda_{1,t}$). The rationale for using $\lambda_{1,t}$ is that these fluctuations are deviations from a statistically stable size structure (Tuljapurkar 1990). Accordingly, these two approaches were qualitatively consistent in that they both revealed large uncertainty in the effects of vital rate correlations on year-to-year variability, with posterior distributions centered near zero. However, the LTRE decomposition of the variance in $\lambda_{1,t}$ showed that mean effect of correlations tended to decrease variance for all three species, while the simulation analysis of variance in λ_t indicated that correlations tended to increase variance in two species with no effect on the third. These differences suggest that fluctuations around the statistically stationary size distribution add noise to λ_t, and therefore weaken the direct effect of fluctuations in vital rates represented by $\lambda_{1,t}$. This finding agrees with two recent comparative studies based on matrix population models, which found that the variance in realized growth rates (λ_t) caused by fluctuations in size structure was often larger than the variance caused by fluctuations in vital rates (Ellis and Crone 2013, McDonald et al. 2016). Our results suggest that the role of transient dynamics in modulating the effect of vital rate correlations on stochastic population dynamics deserves further empirical and theoretical study.

An important caveat of our study is that, despite the long-term nature of our data, our inferences are limited because they are based on only three species with one population each. The geographic limitation of our study may bias our estimates of demographic variation and covariation. The literature increasingly suggests large geographic variation in vital rates across populations of the same species (Doak and Morris 2010, Schindler et al. 2010, Eckhart et al. 2011, Villellas et al. 2015). Given these limitations, it is worth considering how generally we may conclude that vital rate correlations do not meaningfully affect stochastic population dynamics. We intentionally focused on species with similar life histories. Our three focal species share complex iteroparous perennial life histories, including overlapping generations, extended reproductive delays, long-lived reproductive stages, and demographic "storage" in the form of seed banks or dormant stages. We speculate that our conclusions regarding the importance of vital rate correlations may apply broadly to organisms with similarly complex life cycles, where the suite of life history processes operating simultaneously may dilute the importance of any single process or pair of processes. Indeed, our results reinforce previous studies of long-lived plants and animals that found weak effects of vital rate covariation (Jongejans et al. 2010, Morris et al. 2011). At the other, simpler extreme of life cycle complexity, vital rate correlations may be more consequential. For example, in an unstructured population governed solely by birth and death

rates, strong correlation between these two processes may importantly affect population dynamics in a variable environment. These hypotheses regarding the role of life cycle complexity are well suited to theoretical study, which we suggest would be a fruitful area for further work.

Conclusion

In this study, we show that temporal vital rate correlations in three perennial plant species are usually weak but occasionally strong, and in both directions. While vital rate correlations have potential to modify year-to-year variability and thus stochastic population growth, we found that correlations had virtually no effect on stochastic population dynamics and did not modify our inferences of population viability. Explanations for the negligible effects of vital rate correlations may include the predominance of weak correlations, low sensitivities and low variability of the few vital rates that were strongly correlated, and fluctuations in size structure over-riding fluctuations in vital rates. Our results offer potentially good news for population ecologists, because the process of estimating and modeling vital rate correlations is data-intensive and computationally nontrivial.

Literature Cited

Adler, P. B., H. J. Dalgleish, and S. P. Ellner. 2012. Forecasting plant community impacts of climate variability and change: when do competitive interactions matter? Journal of Ecology 100:478–487.

Adler, P. B., J. HilleRisLambers, P. C. Kyriakidis, Q. Guan, and J. M. Levine. 2006. Climate variability has a stabilizing effect on the coexistence of prairie grasses. Proceedings of the National Academy of Sciences USA 103:12793–12798.

Barraquand, F., and N. G. Yoccoz. 2013. When can environmental variability benefit population growth? Counterintuitive effects of nonlinearities in vital rates. Theoretical Population Biology 89:1–11.

Benson, L. 1982. The cacti of the United States and Canada. Stanford University Press, Stanford, California, USA.

Boyce, M., C. Haridas, C. Lee, and The NCEAS Stochastic Demography Working Group. 2006. Demography in an increasingly variable world. Trends in Ecology & Evolution 21:141–148.

Brooks, S. P., and A. Gelman. 1998. General methods for monitoring convergence of iterative simulations. Journal of Computational and Graphical Statistics 7:434–455.

Buckley, Y. M., S. Ramula, S. P. Blomberg, J. H. Burns, E. E. Crone, J. Ehrlén, T. M. Knight, J.-B. Pichancourt, H. Quested, and G. M. Wardle. 2010. Causes and consequences of variation in plant population growth rate: a synthesis of matrix population models in a phylogenetic context. Ecology Letters 13:1182–1197.

Caswell, H. 2001. Matrix population models: construction, analysis, and interpretation. Sinauer Associates, Sunderland, Massachusetts, USA.

Charnov, E. L. 1993. Life history invariants. Oxford University Press, Oxford, UK.

Clark, J. S., D. M. Bell, M. H. Hersh, and L. Nichols. 2011. Climate change vulnerability of forest biodiversity: climate and competition tracking of demographic rates. Global Change Biology 17:1834–1849.

Coulson, T., J.-M. Gaillard, and M. Festa-Bianchet. 2005. Decomposing the variation in population growth into contributions from multiple demographic rates. Journal of Animal Ecology 74:789–801.

Dalgleish, H. J., D. N. Koons, M. B. Hooten, C. A. Moffet, and P. B. Adler. 2011. Climate influences the demography of three dominant sagebrush steppe plants. Ecology 92:75–85.

Davison, R., F. Nicolè, H. Jacquemyn, and S. Tuljapurkar. 2013. Contributions of covariance: decomposing the components of stochastic population growth in *Cypripedium calceolus*. American Naturalist 181:410–420.

Doak, D., P. Kareiva, and B. Klepetka. 1994. Modeling population viability for the desert tortoise in the western Mojave Desert. Ecological Applications 4:446.

Doak, D. F., and W. F. Morris. 2010. Demographic compensation and tipping points in climate-induced range shifts. Nature 467:959–962.

Doak, D. F., W. F. Morris, C. Pfister, B. E. Kendall, and E. M. Bruna. 2005. Correctly estimating how environmental stochasticity influences fitness and population growth. American Naturalist 166:E14–E21.

Duane, S., A. D. Kennedy, B. J. Pendleton, and D. Roweth. 1987. Hybrid Monte Carlo. Physics Letters B 195:216–222.

Easterling, D. R., G. A. Meehl, C. Parmesan, S. A. Changnon, T. R. Karl, and L. O. Mearns. 2000. Climate extremes: observations, modeling, and impacts. Science 289:2068–2074.

Eckhart, V. M., M. A. Geber, W. F. Morris, E. S. Fabio, P. Tiffin, D. A. Moeller, and E. M. A. McPeek. 2011. The geography of demography: long-term demographic studies and species distribution models reveal a species border limited by adaptation. American Naturalist 178:S26–S43.

Elderd, B. D., and T. E. X. Miller. 2016. Quantifying demographic uncertainty: Bayesian methods for integral projection models. Ecological Monographs 86:125–144.

Ellis, M. M., and E. E. Crone. 2013. The role of transient dynamics in stochastic population growth for nine perennial plants. Ecology 94:1681–1686.

Ellner, S. P., and M. Rees. 2006. Integral projection models for species with complex demography. American Naturalist 167:410–428.

Evans, M. E. K., and K. E. Holsinger. 2012. Estimating covariation between vital rates: a simulation study of connected vs. separate generalized linear mixed models (GLMMs). Theoretical Population Biology 82:299–306.

Evans, M. E., K. E. Holsinger, and E. S. Menges. 2010. Fire, vital rates, and population viability: a hierarchical Bayesian analysis of the endangered Florida scrub mint. Ecological Monographs 80:627–649.

Ezard, T. H. G., P. H. Becker, and T. Coulson. 2006. The contributions of age and sex to variation in common tern population growth rate. Journal of Animal Ecology 75:1379–1386.

Fieberg, J., and S. P. Ellner. 2001. Stochastic matrix models for conservation and management: a comparative review of methods. Ecology Letters 4:244–266.

Franco, M., and J. Silvertown. 2004. A comparative demography of plants based upon elasticities of vital rates. Ecology 85:531–538.

Gelman, A., J. B. Carlin, H. S. Stern, D. B. Dunson, A. Vehtari, and D. B. Rubin. 2013. Bayesian data analysis. Third edition. Chapman & Hall/CRC Press, London, UK.

Gelman, A., and J. Hill. 2007. Data analysis using regression and multilevel/hierarchical models. Cambridge University Press, Cambridge, UK.

Harper, J. L. 1977. Population biology of plants. Academic Press, London, UK.

Hoffman, M. D., and A. Gelman. 2014. The No-U-Turn sampler: adaptively setting path lengths in Hamiltonian Monte Carlo. Journal of Machine Learning Research 15:1593–1623.

Hsu, J. S., J. Powell, and P. B. Adler. 2012. Sensitivity of mean annual primary production to precipitation. Global Change Biology 18:2246–2255.

Ibáñez, I., J. A. Silander Jr., A. M. Wilson, N. LaFleur, N. Tanaka, and I. Tsuyama. 2009. Multivariate forecasts of potential distributions of invasive plant species. Ecological Applications 19:359–375.

Inouye, D. W. 2008. Effects of climate change on phenology, frost damage, and floral abundance of montane wildflowers. Ecology 89:353–362.

Jacquemyn, H., and R. Brys. 2010. Temporal and spatial variation in flower and fruit production in a food-deceptive orchid: a five-year study. Plant Biology 12:145–153.

Jacquemyn, H., R. Brys, R. Davison, S. Tuljapurkar, and E. Jongejans. 2012. Stochastic LTRE analysis of the effects of herbivory on the population dynamics of a perennial grassland herb. Oikos 121:211–218.

Jacquemyn, H., R. Brys, and E. Jongejans. 2010. Size-dependent flowering and costs of reproduction affect population dynamics in a tuberous perennial woodland orchid: size-dependent demography in a woodland orchid. Journal of Ecology 98:1204–1215.

Jenouvrier, S., M. Holland, J. Stroeve, C. Barbraud, H. Weimerskirch, M. Serreze, and H. Caswell. 2012. Effects of climate change on an emperor penguin population: analysis of coupled demographic and climate models. Global Change Biology 18:2756–2770.

Jongejans, E., H. De Kroon, S. Tuljapurkar, and K. Shea. 2010. Plant populations track rather than buffer climate fluctuations. Ecology Letters 13:736–743.

Knops, J. M., W. D. Koenig, and W. J. Carmen. 2007. Negative correlation does not imply a tradeoff between growth and reproduction in California oaks. Proceedings of the National Academy of Sciences USA 104:16982–16985.

Lawson, C. R., Y. Vindenes, L. Bailey, and M. van de Pol. 2015. Environmental variation and population responses to global change. Ecology Letters 18:724–736.

Lewandowski, D., D. Kurowicka, and H. Joe. 2009. Generating random correlation matrices based on vines and extended onion method. Journal of Multivariate Analysis 100:1989–2001.

Lewontin, R. C., and D. Cohen. 1969. On population growth in a randomly varying environment. Proceedings of the National Academy of Sciences USA 62:1056–1060.

Lunn, D. J., A. Thomas, N. Best, and D. Spiegelhalter. 2000. WinBUGS – a Bayesian modelling framework: concepts, structure, and extensibility. Statistics and Computing 10: 325–337.

McDonald, J. L., I. Stott, S. Townley, and D. J. Hodgson. 2016. Transients drive the demographic dynamics of plant populations in variable environments. Journal of Ecology 104:306–314.

Miller, T. E. X., S. M. Louda, K. A. Rose, and J. O. Eckberg. 2009. Impacts of insect herbivory on cactus population dynamics: experimental demography across an environmental gradient. Ecological Monographs 79:155–172.

Miller, T. E. X., J. L. Williams, E. Jongejans, R. Brys, and H. Jacquemyn. 2012. Evolutionary demography of iteroparous plants: incorporating non-lethal costs of reproduction into integral projection models. Proceedings of the Royal Society B 279:2831–2840.

Morris, W. F. 1997. Disentangling effects of induced plant defenses and food quantity on herbivores by fitting nonlinear models. American Naturalist 150:299–327.

Morris, W. F., J. Altmann, D. K. Brockman, M. Cords, L. M. Fedigan, A. E. Pusey, T. S. Stoinski, A. M. Bronikowski, S. C. Alberts, and K. B. Strier. 2011. Low demographic variability in wild primate populations: fitness impacts of variation, covariation, and serial correlation in vital rates. American Naturalist 177:E14–E28.

Morris, W. F., and D. F. Doak. 2004. Buffering of life histories against environmental stochasticity: accounting for a spurious correlation between the variabilities of vital rates and their contributions to fitness. American Naturalist 163: 579–590.

Morris, W. F., et al. 2008. Longevity can buffer plant and animal populations against changing climatic variability. Ecology 89:19–25.

Neubert, M. G., and H. Caswell. 1997. Alternatives to resilience for measuring the responses of ecological systems to perturbations. Ecology 78:653–665.

Obeso, J. R. 2002. The costs of reproduction in plants. New Phytologist 155:321–348.

Ohm, J. R., and T. E. X. Miller. 2014. Balancing anti-herbivore benefits and anti-pollinator costs of defensive mutualists. Ecology 95:2924–2935.

Pfister, C. A. 1998. Patterns of variance in stage-structured populations: evolutionary predictions and ecological implications. Proceedings of the National Academy of Sciences USA 95:213–218.

Plummer, M. 2003. JAGS: a program for analysis of Bayesian graphical models using Gibbs sampling. Proceedings of the 3rd International Workshop on Distributed Statistical Computing, Vienna, Austria.

Rahmstorf, S., and D. Coumou. 2011. Increase of extreme events in a warming world. Proceedings of the National Academy of Sciences USA 108:17905–17909.

Reed, A. W., and N. A. Slade. 2006a. Environmental stochasticity: empirical estimates of prairie vole survival with implications for demographic models. Canadian Journal of Zoology 84:635–642.

Reed, A. W., and N. A. Slade. 2006b. Demography and environmental stochasticity: empirical estimates of survival in three grassland rodents. Journal of Zoology 272:110–115.

Rees, M., and S. P. Ellner. 2009. Integral projection models for populations in temporally varying environments. Ecological Monographs 79:575–594.

Roff, D. A. 2002. Life history evolution. Sinauer Associates, Sunderland, Massachusetts, USA.

Rose, F. 1948. Flora of the British Isles: Orchis purpurea Huds. Journal of Ecology 36:366–377.

Ruel, J. J., and M. P. Ayres. 1999. Jensen's inequality predicts effects of environmental variation. Trends in Ecology & Evolution 14:361–366.

Saether, B.-E., and Ø. Bakke. 2000. Avian life history variation and contribution of demographic traits to the population growth rate. Ecology 81:642–653.

Salguero-Gómez, R., et al. 2015. The COMPADRE Plant Matrix Database: an open online repository for plant demography. Journal of Ecology 103:202–218.

Schindler, D. E., R. Hilborn, B. Chasco, C. P. Boatright, T. P. Quinn, L. A. Rogers, and M. S. Webster. 2010. Population diversity and the portfolio effect in an exploited species. Nature 465:609–612.

Schönbrodt, F. D., and M. Perugini. 2013. At what sample size do correlations stabilize? Journal of Research in Personality 47:609–612.

Silvertown, J., and M. Dodd. 1999. The demographic cost of reproduction and its consequences in Balsam Fir (*Abies balsamea*). American Naturalist 154:321–332.

Stan Development Team. 2015. Stan modeling language user's guide and reference manual, Version 2.6.1. http://mc-stan.org/

Stearns, S. S. 1992. The evolution of life histories. Oxford University Press, Oxford, England.

Tuljapurkar, S. D. 1982. Population dynamics in variable environments. III. Evolutionary dynamics of r-selection. Theoretical Population Biology 21:141–165.

Tuljapurkar, S. D. 1990. Population dynamics in variable environments. Springer, Berlin, Germany.

Tuljapurkar, S. D., J.-M. Gaillard, and T. Coulson. 2009. From stochastic environments to life histories and back.

Philosophical Transactions of the Royal Society B 364: 1499–1509.

Tuljapurkar, S. D., and S. H. Orzack. 1980. Population dynamics in variable environments. I. Long-run growth rates and extinction. Theoretical Population Biology 18:314–342.

Vasseur, D. A., J. P. DeLong, B. Gilbert, H. S. Greig, C. D. G. Harley, K. S. McCann, V. Savage, T. D. Tunney, and M. I. O'Connor. 2014. Increased temperature variation poses a greater risk to species than climate warming. Proceedings of the Royal Society B 281:20132612.

Villellas, J., D. F. Doak, M. B. García, and W. F. Morris. 2015. Demographic compensation among populations: What is it, how does it arise and what are its implications? Ecology Letters 18:1139–1152.

Weber, W. A. 1952. The genus *Helianthella* (Compositae). American Midland Naturalist 48:1.

Williams, J. L., H. Jacquemyn, B. M. Ochocki, R. Brys, and T. E. X. Miller. 2015. Life history evolution under climate change and its influence on the population dynamics of a long-lived plant. Journal of Ecology 103:798–808.

Woodward, A., D. G. Silsbee, E. G. Schreiner, and J. E. Means. 1994. Influence of climate on radial growth and cone production in subalpine fir (*Abies lasciocarpa*) and mountain hemlock (*Tsuga mertensiana*). Canadian Journal of Forest Research 24:1133–1143.

SUPPORTING INFORMATION

DATA AVAILABILITY